Can heat flow backward? unusual thermal phenomena observed in near-critical fluids

Daniel Beysens, Yves Garrabos, Régis Wunenburger, Carole Lecoutre-Chabot

Can heat flow backward? Unusual thermal phenomena observed in near-critical fluids

D. Beysens[a,*], Y. Garrabos[b], R. Wunenburger[b], C. Lecoutre[b]

[a] *Equipe du Supercritique pour l'Environnement, les Matériaux et l'Espace, Service des Basses Températures, Département de Recherche Fondamentale sur la Matière Condensée, Commissariat á l'Energie Atomique, 17 rue des Martyrs, 38054 Grenoble Cedex 9, France*

[b] *Equipe du Supercritique pour l'Environnement, les Matériaux et l'Espace, Institut de Chimie de la Matière Condensée de Bordeaux, UPR 9048 Centre National de la Recherche Scientifique, Université Bordeaux I, avenue du Docteur A. Schweitzer, 33608 Pessac Cedex, France*

* Corresponding author. Fax: +33-476-88-51-99.
E-mail address: dbeysens@cea.fr (D. Beysens).

Abstract

A study is presented concerning an experiment under weightlessness. A pure fluid (SF_6) is heated near and below its critical point, where liquid coexists with vapor. After the temperature rise, the vapor phase passes well beyond the temperature of the heating walls. This surprising finding is discussed in the light of an adiabatic heat transfer or "Piston effect" and the special geometry of the liquid and vapor. In addition, the shape of the gas–liquid interface is distorted near the solid wall by the thrust of vapor production ("recoil" force), a precursor to the well-known boiling crisis in heat exchanger.

PACS: 44.30.+v; 05.70.Jk; 05.70.Ln

Keywords: Two-phase heat and mass transfer; Near-critical fluids; Low gravity; Adiabatic compression; Boiling crisis

1. Introduction

During the last 10 years, our understanding of the out-of-equilibrium behavior of near-critical fluids has made considerable progress thanks to several theoretical, experimental and numerical studies. As the liquid–vapor critical point (CP) is approached, many thermodynamic and transport properties of pure fluids exhibit striking

behavior [1]. Notable examples include the divergence of the isothermal compressibility, of the specific heat, as well as the vanishing behavior of the thermal diffusivity and of the surface tension. This makes the near-critical fluids very sensitive to any thermal perturbation, and results in a strong coupling between thermodynamics and hydrodynamics. Microgravity is unique to study the heat and mass transfer processes in near-critical fluids without the influence of neither stratification nor convection. In fluids maintained at constant volume, a new mechanism of heat transfer by thermo-acoustic coupling was observed under microgravity (Ref. [2] and references therein). It was called "piston effect" or "adiabatic heating" because an expanding hot boundary layer acts as a piston to heat the interior of the fluid in an adiabatic manner. This mechanism leads to a very fast thermalization of homogeneous fluid samples. The out-of-equilibrium behavior of near-critical two-phase fluids is more complex to describe, since the fluid is inhomogeneous, and phase change can occur either. In addition, interface motion and deformation caused by the thermal perturbations can modify the phase distribution within the fluid and influence the heat transfer itself.

From the practical point of view, since two-phase heat transfer associated with phase change (called "boiling") usually allows larger amount of heat to be transferred than in a one-phase fluid, it is involved in many types of heat transfer technologies. Under microgravity, the absence of buoyancy that on earth lifts the gas bubbles nucleating on a hot surface makes clearer the study of boiling. The vicinity of the CP is here used as a tool to vary continuously the thermophysical properties of the fluid by simply changing the temperature, taking advantage of the well-known universal power laws of critical phenomena and of the complete wetting of one phase (liquid generally). In a boiling process, we expect that evaporation will dewet the liquid phase from the wall, creating a liquid–gas–solid contact line. The same physics that makes perfect wetting in equilibrium will result in a boundary condition of zero contact angle when heat is applied.

In this paper, we present some curious experimental results on heat and mass transfer in near-critical two-phase fluids induced by temperature changes in microgravity. For this purpose, two different kinds of experiments were performed. The first kind was dedicated to in situ temperature measurements during temperature steps, the second kind to the optical study of the deformation of the liquid–vapor interface occurring when it is in contact with the heating sample cell walls. In Section 2 the experimental apparatus and procedures are presented. In Section 3, paradoxical temperature measurements are reported and discussed. In Section 4, drying of the contact area as observed during heating is presented and its origin discussed.

2. Experimental

These results were obtained using the French ALICE 2 facility on board the Mir station with different fluid samples and different heating protocols during the French/Russian Cassiopée (1996), Pegase (1998), and Perseus (1999) missions, and the French/American GMSF (1999) mission.

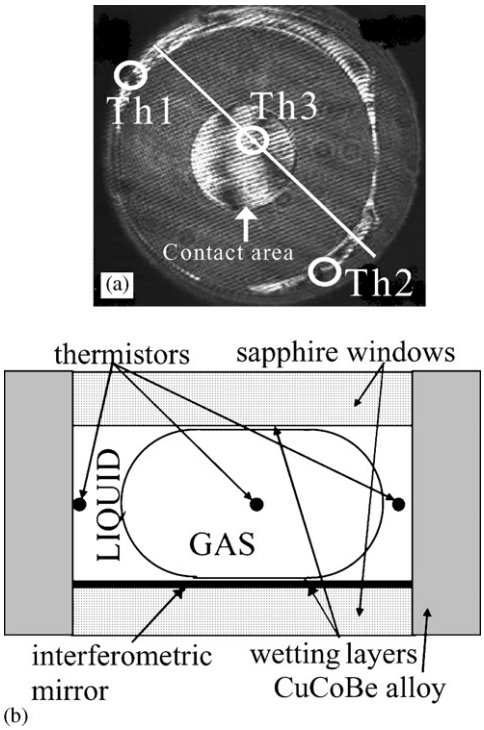

Fig. 1. (a) Interferometric cell (thickness 6.7 mm) used for in situ temperature measurements. White circles: positions of the thermistors. (b) Schematic view of the cell showing the gas and liquid phases.

2.1. Thermal control, measurement, and stimuli

The ALICE 2 facility, whose detailed description is given in Ref. [3], integrates a management system for diagnostics and stimuli with a regulation system that controls the temperature of two sample cells to within a few tens of μK. The experimental cells were imbedded inside a three-stage thermostat. A Yellow Spring Instrument Co. 44900 thermistor (2 s rise time, 100 μK accuracy) imbedded in the sample cell unit (third stage) near the fluid volume was used to follow the temperature evolution of the cell walls (labeled T_W).

The internal fluid volume was a cylinder (12 mm internal diameter, variable thickness) made of high conductivity CuCoBe alloy, sandwiched between two parallel sapphire windows (Fig. 1). Thermal stimuli were either temperature ramps or quenches. In the cells dedicated to temperature measurements, three Thermometrics B10 thermistors (10 ms rise time, 500 μK accuracy, 0.2 mm diameter) were placed in the cell volume, allowing local measurements of the fluid temperature. Two of them (labeled Th1 and Th2) were located close to the cell wall (roughly 1 mm) and were always observed to be in the liquid. The temperatures measured by Th1 and Th2 are labeled T_L^1 and T_L^2. The third thermistor (Th3) was mounted in the center of the cell, so that the gas

bubble, of volume fraction 0.5, was always found to contain thermistor Th3. The temperature measured by Th3 is labeled T_V. The measuring frequencies were 25 Hz for T_L^1, T_L^2 and T_V and 1 Hz for T_W during the first 5 min following a temperature quench, then 0.1 Hz during the next 55 min.

2.2. Optics

The fluid samples were visualized either through light transmission normal to the windows (grid shadow technique [4]) or by differential interferometry (Twyman-Green interferometer, as in Fig. 1a). The image of the samples was recorded by a CCD camera at a frequency of 25 Hz. Since the contact angle is zero near the critical point, the liquid–vapor meniscus between the two parallel windows forms a semi-circular interface in a cross section perpendicular to the windows. The interface appears dark in the images because the liquid–gas meniscus refracts the incident light away from the cell axis.

2.3. Samples

Both pure SF_6 ($T_c = 318.7$ K, $\rho_c = 742$ kg m^{-3}) and CO_2 ($T_c = 304.1$ K, $\rho_c = 467.8$ kg m^{-3}) were used. The interferometric cells were prepared with a high precision density, within 0.2%, by weighing and checking on the ground that the meniscus appears in the middle of the cell after a temperature step below T_c [5]. The initial state of our fluid samples before heating is a flat bubble slightly constrained by the two windows as schematically drawn in Fig. 1b.

2.4. Procedures

In the experiments dedicated to in situ temperature measurement, a series of positive wall step changes in temperature (temperature quench) were performed with $\Delta T = T_f - T_i = 100$ mK and 50 mK for initial temperatures T_i ranging from $T_c - 10.1$ to -0.1 K. A quench of amplitude ΔT consisted in a sharp linear increase of T_W up to 80% of ΔT in less than 10 s, followed by a smooth evolution up to the final temperature T_f.

3. Temperature evolution in liquid and vapor

In this part we present the striking temperature measurements where we observed that vapor temperature was larger than the heating wall temperature. We used a 6.7 mm thick sample that was observed by interferometry (Fig. 1). The evolution of T_W, T_L^1, T_L^2 and T_V during a quench of $\Delta T = +100$ mK from $T_i = T_c - 10.1$ K is shown in Fig. 2. At the beginning of the quench (t= [0–25 s]) all temperatures increased almost linearly in time, with T_L^1, T_L^2 increasing less rapidly than T_V and remaining smaller than T_W. Before the end of the quench, temperature in vapor (T_V) passed strikingly well beyond T_W. Then, T_V decreased slowly up to its final value, T_f. These observations and the vapor-overheating phenomenon can be explained as follows.

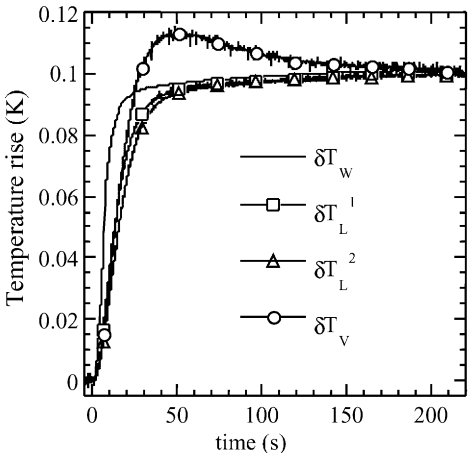

Fig. 2. Temperature rise at the cell wall δT_W, in the liquid δT_L^1 and δT_L^2, and in the vapor δT_V during a quench of amplitude $\Delta T = +0.1$ K from the initial temperature $T_i = T_c - 10.1$ K.

3.1. Initial temperature evolutions

We first compare the initial temperature evolutions in liquid and vapor. During the adiabatic heat transfer process, the increase of pressure due to the expansion of the fluid heated at the boundary can be considered as homogeneous within the sample (the time scales involved here are longer than the time of flight of sound waves). During the short period of efficiency of PE, Onuki and Ferrell [6] pointed out that neither heat nor mass can be transferred between vapor and liquid that are initially at coexistence because the thermal diffusivity is weak near the CP. Consequently, liquid and vapor should behave as if they were independent and the temperature increase in the liquid (δT_L) and the vapor (δT_V) should be homogeneous and isentropic. Here and in the following the rise of any temperature T_X is defined as $\delta T_X = T_X - T_i$. Therefore, in each bulk phase—where "bulk" is defined as the homogeneous fluid region out of the thermal diffusion layers that is heated only by adiabatic compression—the ratio $s = \delta T_V/\delta T_L$ is expected to be

$$s \equiv \frac{\delta T_V}{\delta T_L} = \frac{(\partial(\delta T_V)/\partial t)_{t=0}}{(\partial(\delta T_L)/\partial t)_{t=0}} = \frac{(\partial T/\partial P)_S^V}{(\partial T/\partial P)_S^L} . \quad (1)$$

Since $(\partial T/\partial P)_S^V > (\partial T/\partial P)_S^L$, the vapor should then be more rapidly heated than the liquid, as it is effectively observed (see Fig. 2).

In Fig. 3, the ratios of the temperature growth rates are presented for thermistors Th1 and Th2. The curves are compared to the theoretical prediction (1). Fig. 3 shows that the data are smaller than the expected value from Eq. (1). This disagreement is presumably due to a weak amount of heat and mass exchange occurring between liquid and vapor during the adiabatic compression. Indeed, during the PE heat transfer process, only a thin layer of fluid is able to stay at liquid–vapor coexistence, and the

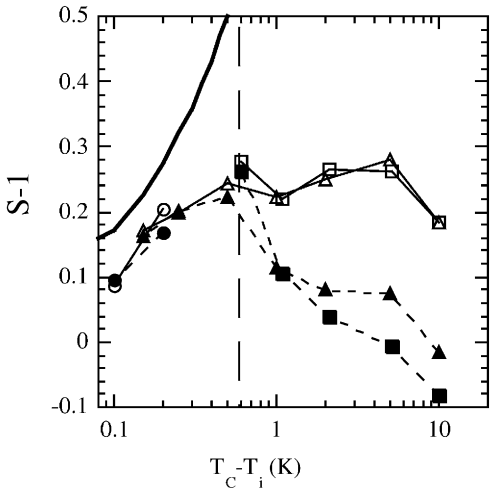

Fig. 3. The initial slopes $(\partial(\delta T_V)/\partial t)/(\partial(\delta T_L^1)/\partial t) - 1$ (solid symbols; dotted line as a guide for the eye) and $(\partial(\delta T_V)/\partial t)/(\partial(\delta T_L^2)/\partial t) - 1$ (open symbols; solid line as a guide for the eye) as a function of $T_c - T_i$. Quench amplitudes: +100 mK (squares), +50 mK (triangles), +25 mK (diamonds), +20 mK (circles). The vertical dashed line separates the regions where Th1 and Th2 are (left) in the liquid bulk and (right) in the liquid hot boundary layer. Bold solid curve: $(\partial T/\partial P)_S^V/(\partial T/\partial P)_S^L - 1$.

temperature difference between the vapor and liquid bulk causes heat and mass flow through the interface, so as to equilibrate the chemical potential near the interface.

The entropy conservation at the interface implies [7]

$$\frac{dm_V}{dt} = \frac{\lambda_V \nabla T_V - \lambda_L \nabla T}{\Delta h}, \tag{2}$$

where dm_V/dt is the rate of vaporization of liquid, Δh the latent heat of vaporization, $\lambda_{V,L}$ are the vapor and liquid thermal conductivity. The contribution $\lambda_V \nabla T_V - \lambda_L \nabla T_L$ represents the heat transported to the interface, which is negative at the beginning of the adiabatic heating. Hence, the adiabatic heating process causes condensation of vapor at the interface at the beginning of the temperature rise. This condensation was numerically observed by Zhong and Meyer [8]. Due to condensation, the vapor is less heated than the liquid, leading to a smaller vapor temperature growth rate than the one deduced from Eq. (1).

3.2. Vapor overheating

We now analyze the vapor-overheating phenomenon. In order to compare the vapor overheating detected during quenches of different amplitudes, the temperature rise in the vapor δT_V was scaled to the temperature rise of the cell walls δT_W, and the behavior of its maximum $(\delta T_V/\delta T_W)_{MAX}$ was plotted as a function of $T_c - T_i$ in Fig. 4. It exhibits a maximum of 123% around $T_c - T_i \approx 5$–7 K. The vanishing differences in thermophysical properties between vapor and liquid at the CP imply that, asymptotically

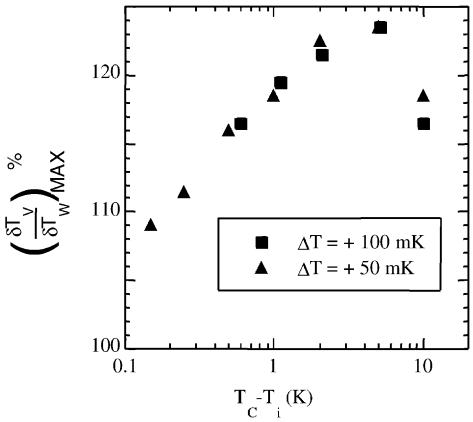

Fig. 4. Vapor overheating as measured by $(\delta T_V/\delta T_W)_{MAX}$, as a function of $T_c - T_i$.

near the CP, vapor and liquid show the same thermal response. On the other hand, far from the CP, the efficiency of the adiabatic heating is reduced and the heat transfer is mainly diffusive, a situation that prevents the vapor overheating. The existence of a maximum for the gas overheating at $T < T_c$ is then due to the competition between these two limiting behaviors.

The occurrence of such a large overheating is due to the geometry of the liquid and vapor phases. Indeed, in this cell, the vapor bubble is almost completely isolated from the thermostated cell walls by the liquid (the area of contact between vapor and windows is less than 6% of the overall heating area). During the quench, the adiabatic heating process stops when T_L^{bulk} has reached T_W (there is not any temperature gradient any more at the boundary). Before the equilibration of T_L^{bulk} and T_W, the bulk vapor is heated more than the bulk liquid by the homogeneous pressure increase. Since the vapor bubble is not in contact with the heating wall, its temperature has no influence on the temperature gradient that drives the expansion of the liquid hot boundary layer (HBL). T_V^{bulk} can thus exhibit a large overshoot. The situation is different on the Earth, where gravity causes the vapor to be in contact with the upper part of the cell. The HBL developing in the vapor stops its expansion when the vapor bulk temperature reaches T_W. When T_V^{bulk} exceeds T_W, the vapor HBL may even contract (cooling piston effect) if the liquid HBL continues to expand in order to compensate vapor overheating. Numerical simulations [8,9] confirmed this influence of the phase distribution on the temperature evolution.

3.3. Vapor temperature relaxation

Finally, the decrease of the vapor temperature down to T_f was found to follow a diffusive law, with the expected thermal diffusivity at this temperature. This behavior is expected, as the PE has stopped and the pressure in the cell remains constant. Details are shown in Ref. [10].

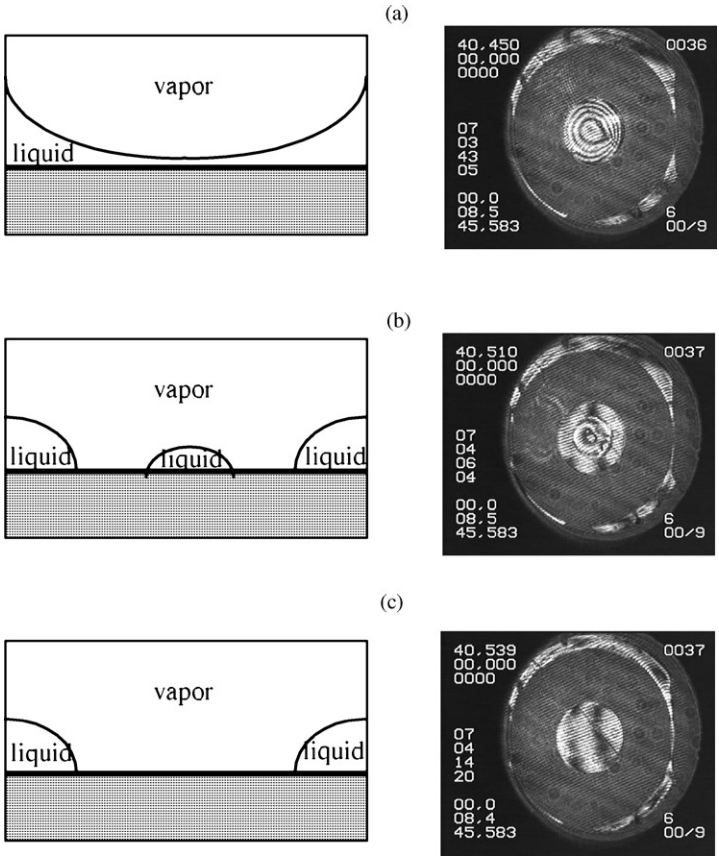

Fig. 5. (a–c) Drying process of the contact region during heating (cell thickness: 6.7 mm). Interferometer pictures (right) and their interpretation (left).

4. Evolution of the contact area

The thickness of the wetting layers is very sensitive to temperature gradients [11]. In the interferometer cell as shown in Fig. 1, the fringes evolution allows the film thickness to be analyzed. A typical evolution is shown in Fig. 5.

Initially, the fringes in the contact area are circular corresponding to a thin wetting layer between the window and the vapor (Fig. 5a). The film is thin because the cell windows compress the vapor bubble (Fig. 1). A calculation [12] gives 12 μm for the minimum film thickness. During the heating period, when the vapor is still colder than the wall, dewetting occurs as a ring (Fig. 5b), with a wet liquid island in the center that eventually dries (Fig. 5c). This drying is well known to those people who deal with the ebullition process, and especially the boiling crisis, when the dry area spreads and that a vapor film isolates the liquid from the heater [13]. A detailed analysis of the drying phenomena is out of the scope of this paper (for more details, see Ref. [14]).

In a different vapor–liquid configuration, when the vapor bubble is pressed against a cell wall, the liquid–vapor interface near the wall is strongly deformed during heating, corresponding to the dewetting and spreading of the dry region [15].

We attribute [15] the drying process above and the dynamical interface deformations observed during sample heating to the presence of a recoil force [16–18], originating from the "thrust" of the vapor that is produced near the liquid–vapor–solid contact line, i.e., the place where the heat flux is maximum.

A very similar drying process takes place during the liquid boiling process at large heat flux. When the heating to a surface is increased past a critical heat flux, there is a sudden transition to "film" boiling, where the heater becomes covered with gas and may burnout [13,16–18]. This "burnout" or "boiling crisis" is an important practical problem in many industries. We interpret the boiling crisis to be similar to the drying transition shown here [18], with the main difference that the interface deformation is made by a large vapor production that can be achieved during strong overheating rather than by the near-critical effects.

5. Conclusion

The striking observation that heat apparently flows backward, from cold to hot, can be understood as the consequence of the transient adiabatic heating process by the Piston effect and the difference in thermophysical properties between liquid and vapor. Not only heat and mass exchange at the interface but also the phase distribution within the cell influence the heat transfer.

Heat and mass transfer in near-critical two-phase fluids are difficult to describe because of the additional adiabatic heat transfer process and the extreme deformability of the liquid–vapor interface. As shown experimentally, the adiabatic heat transfer (Piston effect) in near-critical two-phase fluids leads to an inhomogeneous heat transfer and to the paradoxical overheating of vapor, phenomena that both depend on the phase distribution. The dynamical interface deformations ("drying") observed during temperature ramps is mainly due to the recoil force, at least close to the CP.

Note that a very similar drying takes place during the liquid boiling process at large heat flux. When the heating to a surface is increased past a critical heat flux there is a sudden transition to "film" boiling, where the heater becomes covered with gas and may burnout [15,16].

Acknowledgements

This work was supported by CNES and NASA. We thank Vadim Nikolayev for helpful discussions, R. Nahre for a critical reading of the manuscript.

References

[1] H.E. Stanley, Introduction to Phase Transitions and Critical Phenomena, Clarendon Press, Oxford, 1971.

[2] Y. Garrabos, M. Bonetti, D. Beysens, F. Perrot, T. Fröhlich, P. Carlès, B. Zappoli, Phys. Rev. E 57 (1998) 5665.
[3] R. Marcout, J.F. Zwilling, J.M. Laherrere, Y. Garrabos, D. Beysens, Microgravity Q. 5 (1995) 162.
[4] V. Gurfein, D. Beysens, Y. Garrabos, B. Le Neindre, Opt. Comm. 85 (1991) 147.
[5] C. Morteau, M. Salzman, Y. Garrabos, D. Beysens, in: A. Viviani (Ed.), Proceedings of the Second European Symposium on Fluids in Space, Congressi srl, Roma, 1997, pp. 327–333.
[6] A. Onuki, R.A. Ferrell, Physica A 164 (1990) 245.
[7] A. Onuki, Phys. Rev. A 43 (1991) 6740.
[8] F. Zhong, H. Meyer, Phys. Rev. E 53 (1996) 5935.
[9] R. Wunenburger, Y. Garrabos, C. Lecoutre, D. Beysens, J. Hegseth, F. Zhong, M. Barmatz, Int. J. Thermophys. 23 (2002) 103.
[10] R. Wunenburger, Y. Garrabos, C. Lecoutre-Chabot, D. Beysens, J. Hegseth, Phys. Rev. Lett. 84 (2000) 1400.
[11] R.F. Kayser, J.W. Schmidt, M.R. Moldover, Phys. Rev. Lett. 5 (1985) 707.
[12] R. Wunenburger, Ph.D. Thesis, Université Bordeaux 1, 13 October 2000.
[13] L.S. Tong, Boiling Heat Transfer and Two-Phase Flow, 2nd Edition, Taylor & Francis, New York, 1997.
[14] V.S. Nikolayev, D. Beysens, G.-L. Lagier, J. Hegseth, Int. J. Heat Mass Transfer 44 (2001) 3499.
[15] Y. Garrabos, C. Lecoutre-Chabot, J. Hegseth, V.S. Nikolayev, D. Beysens, J.-P. Delville, Phys. Rev. E 64 (2001) 051602-1, pp. 1–10.
[16] H.J. Palmer, J. Fluid. Mech. 75 (3) (1976) 487.
[17] J. Straub, in: L. Rathe, H. Walter, B. Feuerbacher (Eds.), Proceedings of the IXth European Symposium on Gravity-Dependent Phenomena in Physical Sciences, Springer, Berlin, 1995, pp. 351–359.
[18] V.S. Nikolayev, D. Beysens, Europhys. Lett. 47 (1999) 345.